
DIFF-PIC: Revolutionizing Particle-In-Cell Simulation for Advancing Nuclear Fusion with Diffusion Models

Chuan Liu

University of Rochester

cliu81@ur.rochester.edu

Chunshu Wu

University of Rochester

cuwu88@ur.rochester.edu

Shihui Cao

University of Rochester

sca05@ur.rochester.edu

Mingkai Chen

Rochester Institute of Technology

mxceec@rit.edu

James Chenhao Liang

Rochester Institute of Technology

jcl3689@rit.edu

Ang Li

Pacific Northwest National Laboratory

ang.li@pnnl.gov

Michael Huang

University of Rochester

michael.huang@rochester.edu

Chuang Ren

University of Rochester

chuang.ren@rochester.edu

Dongfang Liu

Rochester Institute of Technology

dongfang.liu@rit.edu

Ying Nian Wu

University of California, Los Angeles

ywu@stat.ucla.edu

Tong Geng*

University of Rochester

tong.geng@rochester.edu

Abstract

Sustainable energy is a crucial global challenge, and recent breakthroughs in nuclear fusion ignition underscore the potential of harnessing energy extracted from nuclear fusion in everyday life, thereby drawing significant attention to fusion ignition research, especially Laser-Plasma Interaction (LPI). Unfortunately, the complexity of LPI at ignition scale renders theory-based analysis nearly impossible – instead, it has to rely heavily on Particle-in-Cell (PIC) simulations, which is extremely computationally intensive, making it a major bottleneck in advancing fusion ignition. In response, this work introduces **DIFF-PIC**, a novel paradigm that leverages conditional diffusion models as a computationally efficient alternative to PIC simulations for generating high-fidelity scientific data. Specifically, we design a distillation paradigm to distill the physical patterns captured by PIC simulations into diffusion models, demonstrating both theoretical and practical feasibility. Moreover, to ensure practical effectiveness, we provide solutions for two critical challenges: ① We develop a physically-informed conditional diffusion model that can learn and generate meaningful embeddings for mathematically continuous physical conditions. This model offers algorithmic generalization and adaptable transferability, effectively capturing the complex relationships between physical conditions and simulation outcomes; and ② We employ the rectified flow technique to make our model a one-step conditional diffusion model, enhancing its efficiency further while maintaining high fidelity and physical validity. DIFF-PIC establishes a new paradigm for using diffusion models to overcome the

*Corresponding author

computational barriers in nuclear fusion research, setting a benchmark for future innovations and advancements in this field.

1 Introduction

Sustainable energy stands as one of the paramount challenges of our era. The recent successful demonstration of fusion ignition [2] underscores the transformative potential of fusion as a sustainable energy source. In 2023 and 2024, the National Ignition Facility (NIF) achieved groundbreaking milestones, generating 3.4 MJ and 5.2 MJ of fusion energy from input energies of 2.2 MJ, respectively. These substantial energy gains emphasize the necessity for a deeper understanding of the fundamental sciences to enhance ignition efficiency. However, the complex and nonlinear nature of Laser-Plasma Interaction (LPI) in physics poses significant challenges for theory-based analysis, necessitating a heavy reliance on Particle-in-Cell (PIC) simulations [64, 35, 61, 5, 39]. Despite being the preeminent standard for modeling the physics of LPI, PIC simulations are exceedingly computationally intensive, often requiring tens of millions of CPU hours and consuming millions of dollars for high-resolution outputs [22, 16, 7]. The computational overhead of PIC simulations has become a bottleneck in fusion research, hindering progress toward the development of practical fusion power plants. Moreover, it is paradoxical that these extensive simulations, which aim to address environmental energy challenges, exacerbate the carbon footprint. Consequently, there is an urgent need for the development of innovative methodologies capable of producing high-quality data with substantially reduced computational burden.

Over the years, numerous CPU-GPU optimizations have been developed to maximize computational efficiency. While these efforts are invaluable, they do not sufficiently address the inherent computational overhead. Recent advancements in generative AI, particularly diffusion models, present a novel approach to these challenges. Diffusion models [56, 24, 59] have demonstrated exceptional capabilities in Computer Vision (CV) [58, 49, 25, 50, 43, 52], synthesizing highly complex and high-dimensional data distributions that match real data with high fidelity. This has sparked significant interest in their potential for generating scientific synthetic data, as recent applications of diffusion models in molecular dynamics simulations have demonstrated their promise in this domain [69, 46].

Theoretically, by distilling the intricate physical patterns captured by PIC simulations into score functions for diffusion models, these models could potentially synthesize complex and high-resolution PIC simulations. In practice, however, the effectiveness of this approach to alleviate the current bottleneck in fusion research remains uncertain. Achieving this goal demands, first of all, that the synthesized data maintain *physical soundness*, and secondly, that there is an *acceleration* in simulation speed compared to conventional PIC methods. Consequently, two critical challenges naturally arise: ① PIC simulations utilize physical conditions as inputs, which differ significantly from the typical inputs in CV tasks, such as text prompts or specific classes. These physical conditions require continuity, meaning the synthesized results must vary smoothly with changes in input conditions. ② Diffusion models generally demand multiple denoising steps to produce high-fidelity data. In this context, it is essential to consider the speedup that diffusion models can provide over traditional PIC simulations while preserving high fidelity.

In light of this perspective, this paper aims to offer the community an alternative to PIC simulations for generating synthetic LPI data and to tackle the two challenges mentioned above. Specifically, we propose an effective and efficient distillation paradigm, titled **DIFF-PIC** (see Fig. 1), that leverages the entire denoising process of diffusion models to generate any arbitrary snapshot produced by PIC simulations. This paradigm treats each snapshot of the system’s evolution as a unique data distribution, thereby enhancing systemic efficiency. To address the first challenge ①, we develop a conditional diffusion model with a physically-informed condition encoder. This encoder allows the conditional diffusion model to learn the relationship between continuous input conditions and generated data, making the physical phenomenon captured by PIC simulation easily distilled to DIFF-PIC. For the second challenge ②, we employ the rectified flow technique to further optimize the runtime efficiency of the proposed conditional diffusion model, demonstrating orders-of-magnitude speedup compared to PIC simulations.

In summary, our work represents the first known effort to tackle the imperative challenges associated with generating high-quality PIC simulation data for LPI using diffusion models. The core contributions of our work include:

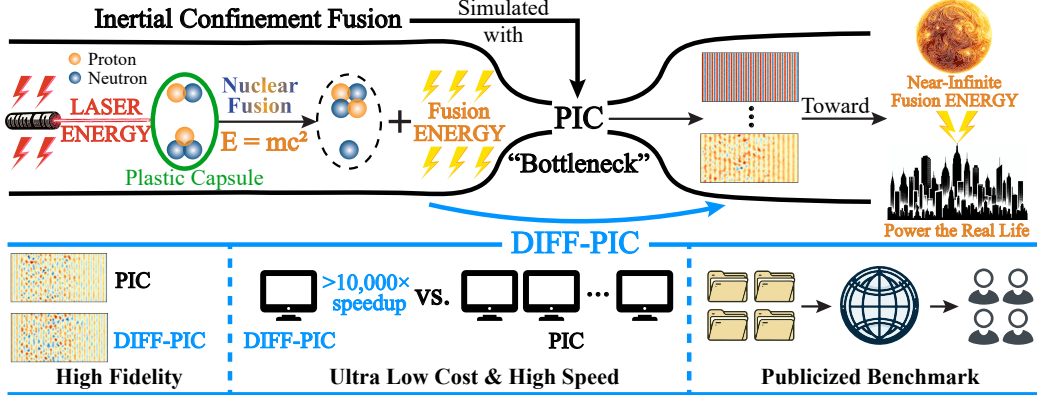


Figure 1: **Overview** of the proposed method.

- We propose **DIFF-PIC**, a pioneering study that utilizes diffusion models as a computationally efficient alternative to PIC simulations for the generation of synthetic data in fusion ignition research (see §3.1). By making all resources publicly available, we aim to establish **DIFF-PIC** as a robust baseline for future improvements and a valuable benchmark for the research community, thereby accelerating the advancement in synthetic data generation for fusion ignition research.
- We develop a physically-informed conditional diffusion model (see §3.2) that seamlessly integrates physical simulation conditions into the diffusion model. The designed condition encoder facilitates the generalization of effective simulation data within and beyond existing simulation parameters, endowing the model with robust generalization capabilities and adaptable transferability.
- We implement the rectified flow technique to transform our model into a one-step diffusion model (see §3.3), thereby enhancing its efficiency in generating high-fidelity fusion data.
- Experimental results in §4.2 demonstrate that our method achieves a remarkable speedup of **16,200** times compared to traditional PIC simulations while preserving high fidelity and physical validity of the generated data, *e.g.*, **0.341**, **34.3**, **8.98e-5** in terms of FID, SWD, and MMD, respectively.

2 Background

Inertial Confinement Fusion (ICF) is a method of achieving nuclear fusion by using intense energy pulses to compress and heat small fuel pellets [28, 9], typically containing isotopes of hydrogen such as deuterium and tritium. This process unfolds the nuclear fusion reaction as delineated below:



Given the ubiquity of these hydrogen isotopes in the ocean, there is immense potential to harness “near-infinite” energy through the study of nuclear fusion. In particular, the goal of the study is to achieve the conditions of temperature and pressure that are sufficient to initiate fusion reactions, and attain a positive net energy gain (*i.e.*, output energy surpassing the input). To optimize the sophisticated initiation of fusion, an advanced understanding of processes is imperative, especially for LPI. For such purposes, PIC is considered a crucial tool to provide theoretical insights into LPI, due to its capability of predicting and interpreting physical phenomena.

Particle-in-Cell Simulations. The PIC method is a computational technique widely used in the study of plasma physics and fusion energy research [64, 47, 11, 27, 16, 53, 48, 68]. Developed in the mid-20th century, the PIC method has become a cornerstone in the simulation of complex plasma behaviors, enabling researchers to delve into the intricate dynamics of particles and electromagnetic fields [36, 37]. To highlight, PIC is especially useful in LPI studies [29, 5, 60, 32, 4]: LPI involves complex dynamics of electrons and ions. PIC simulations track the trajectories and interactions of these charged particles under the influence of electromagnetic fields, providing insights into both shock wave formation, and heating mechanisms that are essential for ICF.

In essence, PIC is an iterative finite element method applied to atomic particles such as electrons and ions. Within each iteration, particles are systematically arranged into discrete cells according to their spatial distribution, with their positions and velocities being updated over infinitesimally small time steps, typically on the scale of femtoseconds (*i.e.*, 10^{-15} seconds). In contrast to molecular

dynamics widely applied in biotechnology [42, 21, 8, 3, 14], PIC simulations in LPI are characterized by the presence of intensive electromagnetic fields, which exert a significant influence on particle trajectories as follows:

$$\frac{d\mathbf{v}_i}{dt} = \frac{q_i}{m_i} (\mathbf{E}(\mathbf{r}_i, t) + \mathbf{v}_i \times \mathbf{B}(\mathbf{r}_i, t)). \quad (2)$$

Consequently, simulating laser-plasma interactions at the scale of even hundreds of Picoseconds (*i.e.*, 10^{-10} seconds) requires the execution of hundreds of thousands of sophisticated PIC iterations. This imposes significant demands on computational storage and processing capabilities. Moreover, the computational complexity of the PIC method can be as high as N^2 for N particles, thereby impeding scalability and computational efficiency. As a result, the PIC methodology has emerged as a stringent bottleneck in fusion research, significantly constraining progress in this domain.

Diffusion models have emerged as a prominent class of generative models within the realm of artificial intelligence, offering an innovative methodology for the synthesis of high-fidelity data [24, 25, 49]. Diverging from traditional generative models such as Generative Adversarial Networks [23] and Variational Autoencoders [31], diffusion models are named after the concept of diffusion in physics. These models are grounded in the principles of stochastic processes, particularly exploiting the notion of diffusion to conceptualize data generation and transformation.

Diffusion models function on the principle of simulating a diffusion process that progressively transforms simple, structured data into a complex distribution and vice versa. The core idea involves two main processes: (1) The Forward Process (Diffusion). In this process, Gaussian noise is gradually added to the data over a series of time steps, transforming the original data distribution into a tractable Gaussian distribution. Mathematically, this can be represented as:

$$q(\mathbf{x}_t | \mathbf{x}_{t-1}) = \mathcal{N}(\mathbf{x}_t; \sqrt{\alpha_t} \mathbf{x}_{t-1}, (1 - \alpha_t) \mathbf{I}), \quad (3)$$

where α_t regulates the noise level at each time step t . (2) The Reverse Process (Denoising). The objective of the reverse process is to reconstruct the original data from the noisy distribution by iteratively denoising the data. This denoising procedure is typically parameterized by a neural network, which is trained to approximate the inverse of the forward diffusion process:

$$p_\theta(\mathbf{x}_{t-1} | \mathbf{x}_t) = \mathcal{N}(\mathbf{x}_{t-1}; \mu_\theta(\mathbf{x}_t, t), \Sigma_\theta(\mathbf{x}_t, t)), \quad (4)$$

where μ_θ represent the mean predicted by the neural network and Σ_θ are untrained time dependent constants. Given their capacity to learn and represent data distributions, diffusion models hold significant promise for synthesizing data derived from Particle-In-Cell (PIC) simulations with enhanced speed and energy efficiency.

3 DIFF-PIC

This section introduces **DIFF-PIC**, a novel physically-informed conditional diffusion model tailored for generating high-fidelity synthetic data for fusion ignition research. As illustrated in Fig. 2, this paradigm conceptualizes each arbitrary snapshot in PIC simulations as a sample from a separate distribution, utilizing the denoising mechanism of diffusion models to predict an arbitrary snapshot $\mathcal{X}(t_{as})$ within the system's evolution. Subsequently, we delve into the *Physically-Informed Condition Encoder*, crafted to tackle the physic condition encoding challenge in this context. Lastly, the *Rectified Flow Acceleration* technique is employed, significantly accelerating the denoising process and thereby enhancing the efficacy of the proposed conditional diffusion model.

3.1 The Overall Distillation Paradigm

By extending the power of diffusion models to PIC simulations, we aim to distill the physical phenomena captured by PIC simulations into diffusion models. This distilling process enables the diffusion model to learn and replicate the complex behaviors and patterns observed in PIC simulations, providing a powerful tool for generating high-fidelity synthetic data in nuclear fusion research.

Concretely, we propose a distillation paradigm as follows: under a specified condition set θ , using the entire denoising process of diffusion models to predict an arbitrary snapshot $\mathcal{X}(t_{as})$ of the system's evolution, each representing a unique data distribution. t_{as} specifies the simulation time step, different from the denoising step t . Therefore, our goal is to learn:

$$\mathcal{X}(t_{as}) = U(\epsilon | t_{as}, \theta). \quad (5)$$

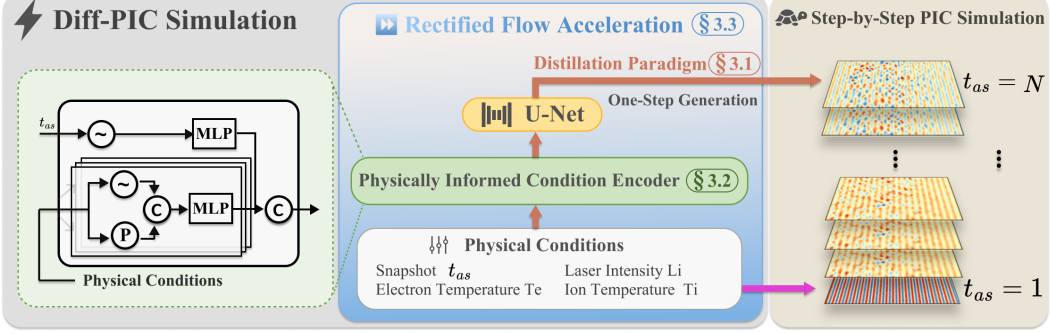


Figure 2: **Pipeline** of the proposed DIFF-PIC.

With U , a diffusion model utilizing the vanilla U-Net for mapping Gaussian noise $\epsilon \sim \mathcal{N}(0, 1)$ to $\mathcal{X}(t_{as})$ under the simulation conditions of θ . Particularly, conditions θ encompass variables including “Electron Temperature,” “Ion Temperature,” and “Laser Intensity,” allowing the model to generate $\mathcal{X}(t_{as})$, detailing the dynamics of each particle, alongside their electric fields at t_{as} .

To train the diffusion model, we construct a dataset of PIC simulation snapshots spanning various simulation conditions. Once trained, the diffusion model can generate synthetic snapshots of the system’s evolution at any desired time and under different physical conditions. These generated snapshots can be used for multiple purposes, including data augmentation, parameter exploration, and studying the effects of different physical conditions. Furthermore, the diffusion model aids in the interpretation and visualization of complex plasma phenomena, providing valuable insights for researchers in the field of nuclear fusion. Essentially, the proposed techniques offers two advantages:

- *Data Dependency Relaxation*. By treating different snapshots under various condition combinations as separate distributions, we can sparsely sample across a specified range of conditions (see §S1c). This approach reduces data dependency for model training, enabling the model to efficiently learn from a limited number of simulations while generalizing across a wide array of scenarios.
- *Systemic efficiency*. Unlike PIC simulations, which generate data sequentially over time, the proposed diffusion model can directly produce data for any target snapshot (see Fig. 3). This non-sequential behavior allows for more efficient data generation and analysis (see Table 4), enabling researchers to focus on specific times of interest without needing to simulate the entire LPI process.

3.2 Physically-Informed Condition Encoder

PIC simulations employ diverse physical conditions as inputs, which necessitate a seamless and continuous transition in the resulting synthesized data as these input conditions vary. Therefore, the condition encoder plays a crucial role, responsible for transforming domain-specific inputs into embeddings comprehensible by the model. These inputs comprise the simulation conditions θ and the target simulation time step t_{as} that the conditional diffusion model aims to generate.

Given the extensive potential range of simulation conditions and the limited data available during training, an optimal encoder must excel in both *interpolation* and *extrapolation* — critical measures of the model’s generalizability. Recall that interpolation capability refers to the encoder’s proficiency in generating suitable embeddings for new conditions that, although not encountered during training, lie between two observed conditions. Extrapolation capability, conversely, pertains to generating embeddings for conditions that fall outside the range of those observed during training. Both capabilities are indispensable for addressing the LPI problem.

To meet the two essentials, we introduce a Physically-Informed Condition Encoder (PICE) to encode the simulation conditions θ , incorporating two distinct types of encoders. For interpolation, we employ Positional Encoding [65] to learn a continuous representation of input conditions, enabling smooth transitions between observed conditions. To augment extrapolation capability, we enhance the encoder with a polynomial architecture, utilizing transformation functions constructed as a linear combination of polynomial basis functions $f_i(\theta)$ of varying degrees:

$$\mathcal{P}(\theta) = \sum_{i=0}^n f_i(\theta), \quad (6)$$

where n denotes the maximum degree, and $\mathcal{P}(\theta)$ can be chosen as Chebyshev polynomials, or Legendre polynomials, based on the characteristics of the condition space. This polynomial enhancement

allows the encoder to generate plausible embeddings for conditions well beyond those encountered during training, ensuring robust performance across a broader spectrum of simulation scenarios. Subsequently, we concatenate the embeddings from these two encoders and apply a Multi-Layer Perceptron (MLP) to further refine the embeddings. The MLP, with its trainable parameters, learns to combine and transform the concatenated embeddings, resulting in a more informative representation of the input conditions. For encoding the simulation time step t_{as} , we utilize Positional Encoding [65] followed by an MLP layer. This approach is specifically chosen to learn continuous representations that facilitate smooth transitions between consecutive time steps, thereby enhancing the model’s temporal coherence. In summary, this design offers the following advantages:

- *Algorithmic generalization.* PICE improves the generalizability of the conditional diffusion model (see Table 2). The dual-encoding strategy leverages spatial information and captures non-linear relationships by incorporating both positional and polynomial encodings, empowering the model to adeptly manage a diverse array of simulation conditions, ranging from scenarios encountered during the training phase to conditions that lie beyond the spectrum of the training data.
- *Adaptable transferability.* The PICE framework significantly augments our model’s adaptability to diverse physical scenarios and boundary conditions (see Table 2). By fine-tuning the pre-trained model with a minimal dataset, this methodology facilitates seamless adaptation, rendering our approach highly applicable across various domains within fusion research and other fields where precise and efficient simulations are imperative for deciphering intricate physical phenomena.

3.3 Rectified Flow-Based Acceleration

To enable rapid generation of high-fidelity synthetic data, we employ the Rectified Flow Acceleration (RFA) technique in model optimization. RFA leverages the principles of rectified flow [40, 18, 41] to convert the complex data trajectory from initial noise ϵ to the target snapshot $\mathcal{X}(t_{as})$ into a single streamlined denoising step, specifically aiming to distill the typically winding diffusion path into a direct and straight path — the shortest route between two distributions. During training, RFA minimizes the following objective function with straight ordinary differential equations:

$$\arg \min_{\zeta} \mathbb{E} \left[\int_0^1 \|(\mathcal{X}(t_{as}) - \epsilon) - \zeta(\mathcal{X}_t, t \mid t_{as}, \theta)\|^2 dt \right], \quad (7)$$

where $\mathcal{X}_t = t\mathcal{X}(t_{as}) + (1-t)\epsilon$ denotes the linear interpolation between $\mathcal{X}(t_{as})$ and ϵ across the diffusion timeline, with t ranging from 0 to 1. The score-based model ζ , approximated using the U-Net, defines the learned trajectory. By minimizing the expectation of the squared deviations between the straight path $\mathcal{X}(t_{as}) - \epsilon$ and the learned trajectory $\zeta(\mathcal{X}_t, t \mid t_{as}, \theta)$, RFA promotes the adoption of the shortest and most direct path in the transformation process, thus significantly reducing the denoising time. Once this time-dependent score-based model ζ is trained, we further straighten the learned trajectories through an interactive reflow procedure [41]. In summary, the RFA module provides additional benefits for our paradigm:

- *Streamlined Denoising Process.* RFA significantly accelerates the denoising process (see Table 4) by converting the complex data trajectory from initial noise to the target snapshot into a direct denoising step. By distilling the typically winding diffusion path into the shortest route between two distributions, RFA greatly reduces the time required for generating high-fidelity synthetic data.
- *Robust Optimization.* RFA leverages the principles of rectified flow to minimize deviations between the winding data trajectory and the optimal, shortest path. This direct path approach reduces the possibility of error accumulation that can occur with more winding, iterative methods.

4 Evaluation

4.1 Experimental Setup

Datasets. We provide a novel dataset comprising 6,615 simulations across varied physical conditions, each containing 80 snapshots of electric fields along two orthogonal directions denoted E1 and E2. The data were generated by OSIRIS [19], a well-established PIC simulation software suite. The dataset covers diverse conditions, including Electron Temperature (Te), Ion Temperature (Ti), and Laser Intensity (Li), all of which are critical parameters influencing particle dynamics and the resultant electric fields. To foster further advancements in fusion research, we will release the dataset publicly upon acceptance.

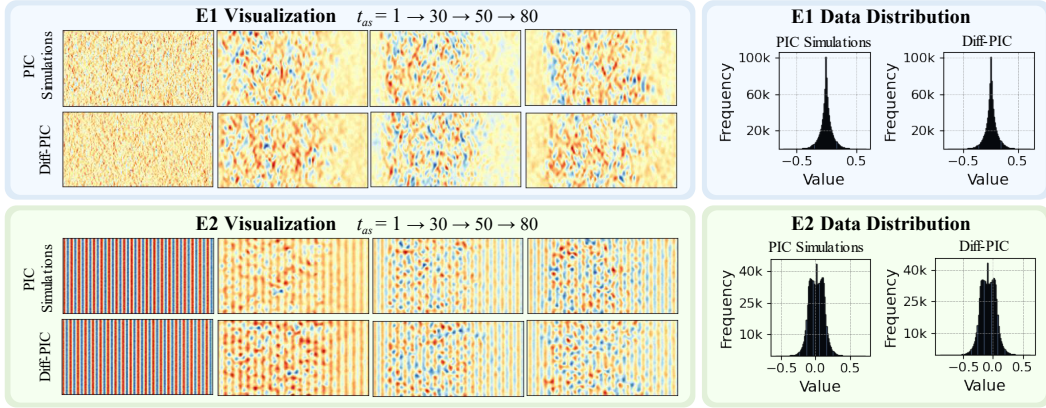


Figure 3: **Visualization and Comparison** of PIC simulations and DIFF-PIC.

Table 1: **Quantitative results** for interpolation evaluation.

Method	Training Set for E1			Testing Set for E1			Training Set for E2			Testing Set for E2		
	FID↓	SWD↓	MMD↓	FID↓	SWD↓	MMD↓	FID↓	SWD↓	MMD↓	FID↓	SWD↓	MMD↓
B-1	1.59	41.2	5.33e-4	1.87	46.8	7.21e-4	0.438	27.5	2.45e-4	0.513	37.6	2.89e-4
B-2	1.28	33.9	2.93e-4	1.54	44.3	5.11e-4	0.324	25.6	7.82e-5	0.336	35.2	9.13e-5
DIFF-PIC	1.21	37.7	3.06e-4	1.62	40.4	5.35e-4	0.328	25.1	7.61e-5	0.341	34.3	8.98e-5

Metrics. To evaluate the quality of the data synthesized by DIFF-PIC, three metrics are adopted for comprehensive comparisons, including Fréchet Inception Distance (FID), Sliced Wasserstein Distance (SWD), and Maximal Mean Discrepancy (MMD). To validate physical soundness, Mean Absolute Error (MAE) and Root Mean Squared Error (RMSE) are used to evaluate the energy difference between the synthetic physical environment and the ground truth.

Baselines. As there are few related studies to compare with, we evaluate two baselines as two design variations to demonstrate the effectiveness and speed of DIFF-PIC. The first baseline (**B-1**), replaces the designed PICE with a simple MLP encoder, which is then integrated with the diffusion model. The second baseline (**B-2**), is a version of DIFF-PIC that uses 1000 denoising steps through the DDPM noise scheduler [24]. These baselines help to highlight the contributions of the key components in the DIFF-PIC architecture.

4.2 Main Results

In this section, we evaluate DIFF-PIC on three key aspects for comprehensive comparisons. (1) The ability to interpolate and extrapolate data with novel physical conditions. (2) The physical validity of the synthetic physical environment. (3) The speedup and power efficiency compared to traditional PIC simulations. As a teaser, Fig. 3 compares the electric field results across 80 snapshots produced by DIFF-PIC and PIC respectively in the testing set. The distributions on the right demonstrate that our proposed model successfully captures the data distributions in the ground truths.

Interpolation and Extrapolation. The interpolation evaluation is carried out for a range of physical conditions (*i.e.*, Te, Ti and Li). Among the conditions, 700 condition configurations are sampled, with 80% partitioned for training and the remaining 20% for testing. In Table 1, the remarkably low FID, SWD, and MMD scores indicate that the proposed DIFF-PIC is able to synthesize high-quality scientific data similar to what PIC generates, meanwhile significantly outperforming baseline B-1 (*i.e.*, without physically-informed conditional encoder equipped) on all three metrics. Compared to baseline B-2, the variations in scores are marginal, likely due to minor fluctuations in evaluation.

In terms of extrapolation, the capability of DIFF-PIC is demonstrated with the electric field results on two orthogonal directions in Table 2 and Table 3. In the experiments, we progressively extend the range of physical conditions from the range selected for training. Specifically, the ranges are extended by 10%, 20%, 40%, and 80%. Similar to interpolation, the high quality remains for extrapolation, with considerable improvement from baseline B-1.

Table 2: **Quantitative results** for extrapolation evaluation on **E1**.

Method	10%			20%			40%			80%		
	FID \downarrow	SWD \downarrow	MMD \downarrow	FID \downarrow	SWD \downarrow	MMD \downarrow	FID \downarrow	SWD \downarrow	MMD \downarrow	FID \downarrow	SWD \downarrow	MMD \downarrow
B-1	3.92	81.7	3.27e-3	4.64	88.5	3.51e-3	5.25	91.0	4.36e-3	6.14	96.3	9.58e-3
B-2	3.51	78.3	2.64e-3	4.18	87.6	3.11e-3	4.74	89.4	3.96e-3	5.65	94.2	6.17e-3
DIFF-PIC	3.87	81.2	2.76e-3	4.17	87.9	3.05e-3	4.96	90.5	3.91e-3	5.74	95.1	6.24e-3

Table 3: **Quantitative results** for extrapolation evaluation on **E2**.

Method	10%			20%			40%			80%		
	FID \downarrow	SWD \downarrow	MMD \downarrow	FID \downarrow	SWD \downarrow	MMD \downarrow	FID \downarrow	SWD \downarrow	MMD \downarrow	FID \downarrow	SWD \downarrow	MMD \downarrow
B-1	1.94	47.3	7.72e-4	2.03	51.1	7.82e-4	2.19	60.8	8.64e-4	2.57	65.4	9.43e-4
B-2	1.73	44.3	7.28e-4	1.82	47.6	7.36e-4	2.01	52.2	7.83e-4	2.35	62.7	8.84e-4
DIFF-PIC	1.81	47.5	7.34e-4	1.88	47.9	7.41e-4	1.93	51.9	7.76e-4	2.16	60.3	8.79e-4

Physical Validity. In addition to the high quality of the synthetic data, we test the physical validity of the generated electric fields at each snapshot with energy, a fundamental concept used to describe the general property of a physical system. In particular, the energy results of electric fields are illustrated in Fig. 4. We observe that the pattern of the ground truth is captured by DIFF-PIC, with fairly low MAE and RMSE incurred. Especially, for electric field E2, the oscillation in energy is properly preserved in the synthetic data. Furthermore, this evaluation highlights that DIFF-PIC is capable of generating sequentially continuous data, demonstrating the effectiveness of the proposed distillation paradigm and the physically-informed condition encoder.

Speedup and Power Efficiency. In addition to the traditional PIC approach, B-1 and B-2 are also included in the comparison shown in Table 4. The PIC simulations are run on the Perlmutter supercomputer in the National Energy Research Scientific Computing (NERSC) facility, with AMD EPYC 7763 CPUs. As essential fusion phenomena typically appear at approximately 100 ps, the costs of PIC simulation at 100 ps are selected as the reference across the comparisons. The GPU results for DIFF-PIC and baselines B-1 and B-2 are obtained on an Nvidia RTX 4090 GPU to demonstrate the availability of this approach to general users. The CPU results for these approaches are acquired on an Intel 13th Gen i9-13900KF CPU. The results highlight that DIFF-PIC-GPU achieves over $10^4 \times$ speedup versus traditional PIC simulation, as well as $10^4 \times$ in terms of reduced energy cost.

4.3 Discussion

To provide further insights and highlight the value of this work, it is worth noting that our approach exhibits outstanding scalability compared to traditional PIC simulations. In PIC, for N particles, the computing complexity can reach a formidable N^2 , as each particle interacts with every other particle. On the contrary, DIFF-PIC focuses on the macroscopic data (e.g., electric field) in the form of distribution, therefore it is not sensitive to the number of particles in space. For larger particle spaces, the speedup achieved by DIFF-PIC can be easily improved by extra orders of magnitude, further accelerating the research of fusion, or other research areas involving large-scale PIC simulations.

5 Related Work

Particle-in-Cell Simulations have long been fundamental to modeling physical processes in fusion research [63, 20]. However, the computational intensity of PIC simulations presents significant challenges [66]. To mitigate these computational constraints, various methods have explored GPU and hybrid CPU-GPU acceleration technologies. Studies such as [1, 12, 15, 33, 62] have utilized parallel computing, high memory bandwidth, and multiple processors to expedite simulations. Architecturally, the simulator optimized for the Kepler GPU architecture, as discussed in [54], underscores the potential of specific GPU architectures to enhance simulation efficiency. For more intricate simulations, research efforts like [70, 13] have developed hybrid CPU-GPU implementations, [67] introduced a hybrid approach for multi-core and multi-GPU systems, highlighting the continuous integration and evolution of these technologies in advancing PIC simulations. Despite these advancements, these approaches remain reliant on the fundamental PIC framework, which may not completely address the computational burden due to the inherent algorithmic complexity of the PIC method. In recent years, rapid advancements in deep learning have opened new pathways for accelerating scientific

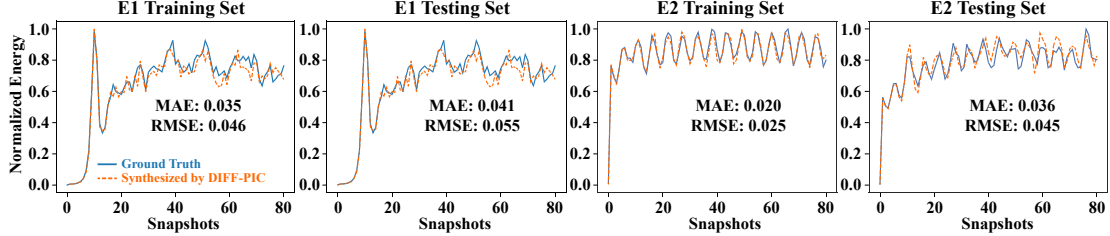


Figure 4: **Energy evaluation** of electric fields for training and test sets with 80 snapshots.

Table 4: **Speedup and Energy Consumption Reduction.**

Method	PIC-100ps	DIFF-PIC-GPU	DIFF-PIC-CPU	B-1-GPU	B-1-CPU	B-2-GPU	B-2-CPU
Speedup	1.00×	1.62e4×	519×	1.66e4×	622×	9.63×	0.550×
Energy Reduction	1.00×	1.01e4×	1.05e3×	1.03e4×	1.26e3×	6.04×	1.11×

simulations. Machine learning-based approaches have emerged, such as predicting a vector space that approximates the PIC system solution [34], and learning the probability of interactions between potential collision pairs [10]. However, the approach by [34] depends on a pre-computed vector space and may not generalize well to novel scenarios, while [10]’s method focuses on binary interactions, overlooking the complex many-body interactions in PIC simulations.

Contrastingly, our proposed method overcomes these limitations by employing a conditional diffusion model to distill the complex patterns captured by PIC simulations from a limited training dataset. Utilizing a time-dependent score-based model, our approach can efficiently generate high-fidelity synthetic data (see Fig. 3 and Table 1) without the computational expense of traditional PIC algorithms (see Table 4). This results in a significant reduction in computational cost while maintaining high simulation accuracy. Moreover, our method is highly adaptable, as it can be fine-tuned with minimal additional data to suit various physical conditions (see Table 2 and 3). This flexibility renders our approach suitable for a wide range of applications in fusion research and beyond, where efficient and accurate simulations are crucial for understanding complex physical phenomena.

Diffusion Models in Scientific Research have emerged as a formidable tool across a myriad of scientific domains. These models, which employ a stochastic process to incrementally convert a pristine data sample into a noise-distributed version and subsequently reverse this process. For instance, in materials science and chemistry, [69] introduced a diffusion model for molecular dynamics simulations, demonstrating the generalizability in generating molecular trajectories. [6] presented an approach that integrates diffusion models with coarse-grained molecular dynamics to develop a new force field for simulating protein dynamics. By leveraging score-based generative models, they trained a model on coarse-grained structures to produce a force field that enhances the performance and realism of protein simulations without requiring force inputs during training. [17] introduced an object-aware SE(3)-equivariant diffusion model for rapidly generating accurate 3D transition state structures, significantly reducing the computational burden typically associated with quantum chemistry calculations. In astrophysics, diffusion models have been utilized to generate synthetic observations and simulate complex astrophysical phenomena. [55] proposed a diffusion model for generating realistic galaxy images, aiding in the analysis of large-scale sky surveys. Diffusion models have also found applications in climate science and Earth system modeling. For instance, [44] employed a deep generative model to super-resolve spatially correlated multiregional climate data, enhancing the spatial resolution of global climate simulations, which is crucial for long-term climate projections and infrastructure development planning. [38] explored the generative emulation of weather forecast ensembles with diffusion models, illustrating their effectiveness as scalable and cost-efficient alternatives to traditional ensemble forecasts, thus improving the reliability and accuracy of predictions for extreme weather events. In particle physics, [26] introduced a diffusion model for generating high-quality Liquid Argon Time Projection Chamber (LArTPC) images, showcasing the model’s ability to handle the challenges of sparse but locally dense particles.

While these studies highlight the expanding interest and application of diffusion models across various scientific domains, their potential within fusion research, specifically as an alternative to PIC simulations, remains underexplored. Our work aims to bridge this gap by proposing DIFF-PIC, a conditional diffusion model that integrates the capability of PIC for generating high-fidelity synthetic

data in fusion research. DIFF-PIC leverages the inherent advantages of diffusion models to provide a computationally efficient alternative to traditional PIC simulations (see Table 4).

6 Conclusions

This paper presents **DIFF-PIC**, a pioneering approach that leverages the capabilities of diffusion models to generate high-fidelity synthetic data for LPI, offering a computationally efficient alternative to conventional PIC simulations in fusion ignition research. By integrating a Physically-Informed Condition Encoder and applying the Rectified Flow Acceleration, DIFF-PIC significantly augments the diffusion model's capacity to manage diverse experimental conditions, thereby expediting the generation of high-fidelity synthetic data. These advancements facilitate rapid, resource-efficient exploration of the design space, markedly diminishing the computational demands associated with PIC simulations. Our research not only catalyzes accelerated scientific discoveries within the realm of fusion research but also sets a novel precedent for the application of generative AI models in scientific simulations. Future investigations may focus on optimizing the distillation paradigm, harmonizing the simulation time t_{as} with the diffusion time t , and refining the condition encoder to encompass a broader spectrum of physical conditions.

References

- [1] Abreu, P., Fonseca, R.A., Pereira, J.M., Silva, L.O.: Pic codes in new processors: A full relativistic pic code in cuda-enabled hardware with direct visualization. *IEEE Transactions on Plasma Science* **39**(2), 675–685 (2010)
- [2] Abu-Shwareb, H., Acree, R., Adams, P., Adams, J., Addis, B., Aden, R., Adrian, P., Afeyan, B., Aggleton, M., Aghaian, L., et al.: Achievement of target gain larger than unity in an inertial fusion experiment. *Physical Review Letters* **132**(6), 065102 (2024)
- [3] Aksimentiev, A., Brunner, R., Cohen, J., Comer, J., Cruz-Chu, E., Hardy, D., Rajan, A., Shih, A., Sigalov, G., Yin, Y., et al.: Computer modeling in biotechnology: a partner in development. *Nanostructure Design: Methods and Protocols* pp. 181–234 (2008)
- [4] Amsden, A.A.: Particle-in-cell method for the calculation of the dynamics of compressible fluids. Tech. rep., Los Alamos National Lab.(LANL), Los Alamos, NM (United States) (1966)
- [5] Arber, T., Bennett, K., Brady, C., Lawrence-Douglas, A., Ramsay, M., Sircombe, N.J., Gillies, P., Evans, R., Schmitz, H., Bell, A., et al.: Contemporary particle-in-cell approach to laser-plasma modelling. *Plasma Physics and Controlled Fusion* **57**(11), 113001 (2015)
- [6] Arts, M., Satorras, V.G., Huang, C.W., Zuegner, D., Federici, M., Clementi, C., Noé, F., Pinsler, R., van den Berg, R.: Two for one: Diffusion models and force fields for coarse-grained molecular dynamics (2023)
- [7] Bastrakov, S., Donchenko, R., Gonoskov, A., Efimenko, E., Malyshev, A., Meyerov, I., Surmin, I.: Particle-in-cell plasma simulation on heterogeneous cluster systems. *Journal of Computational Science* **3**(6), 474–479 (2012)
- [8] Berendsen, H.J.: Bio-molecular dynamics comes of age. *Science* **271**(5251), 954–954 (1996)
- [9] Betti, R., Hurricane, O.: Inertial-confinement fusion with lasers. *Nature Physics* **12**(5), 435–448 (2016)
- [10] Bilbao, P., Badiali, C., Cruz, F.: Towards deep learning accelerated particle-in-cell simulations: application to compton scattering. *OSIRIS* **10**, 3 (2022)
- [11] Birdsall, C.K.: Particle-in-cell charged-particle simulations, plus monte carlo collisions with neutral atoms, pic-mcc. *IEEE Transactions on plasma science* **19**(2), 65–85 (1991)
- [12] Burau, H., Widera, R., Hönig, W., Juckeland, G., Debus, A., Kluge, T., Schramm, U., Cowan, T.E., Sauerbrey, R., Bussmann, M.: Picongpu: a fully relativistic particle-in-cell code for a gpu cluster. *IEEE Transactions on Plasma Science* **38**(10), 2831–2839 (2010)

[13] Chen, G., Chacón, L., Barnes, D.C.: An efficient mixed-precision, hybrid cpu–gpu implementation of a nonlinearly implicit one-dimensional particle-in-cell algorithm. *Journal of Computational Physics* **231**(16), 5374–5388 (2012)

[14] Das, S., Bora, N., Rohman, M.A., Sharma, R., Jha, A.N., Roy, A.S.: Molecular recognition of bio-active flavonoids quercetin and rutin by bovine hemoglobin: an overview of the binding mechanism, thermodynamics and structural aspects through multi-spectroscopic and molecular dynamics simulation studies. *Physical Chemistry Chemical Physics* **20**(33), 21668–21684 (2018)

[15] Decyk, V.K., Singh, T.V.: Adaptable particle-in-cell algorithms for graphical processing units. *Computer Physics Communications* **182**(3), 641–648 (2011)

[16] Derouillat, J., Beck, A., Pérez, F., Vinci, T., Chiaramello, M., Grassi, A., Flé, M., Bouchard, G., Plotnikov, I., Aunai, N., et al.: Smilei: A collaborative, open-source, multi-purpose particle-in-cell code for plasma simulation. *Computer Physics Communications* **222**, 351–373 (2018)

[17] Duan, C., Du, Y., Jia, H., Kulik, H.J.: Accurate transition state generation with an object-aware equivariant elementary reaction diffusion model (2023)

[18] Esser, P., Kulal, S., Blattmann, A., Entezari, R., Müller, J., Saini, H., Levi, Y., Lorenz, D., Sauer, A., Boesel, F., et al.: Scaling rectified flow transformers for high-resolution image synthesis. *arXiv preprint arXiv:2403.03206* (2024)

[19] Fonseca, R.A., Silva, L.O., Tsung, F.S., Decyk, V.K., Lu, W., Ren, C., Mori, W.B., Deng, S., Lee, S., Katsouleas, T., et al.: Osiris: A three-dimensional, fully relativistic particle in cell code for modeling plasma based accelerators. In: *Computational Science—ICCS 2002: International Conference Amsterdam, The Netherlands, April 21–24, 2002 Proceedings, Part III* 2. pp. 342–351. Springer (2002)

[20] Garrigues, L., Fubiani, G., Boeuf, J.P.: Negative ion extraction via particle simulation for fusion: critical assessment of recent contributions. *Nuclear Fusion* **57**(1), 014003 (2016)

[21] Geng, H., Chen, F., Ye, J., Jiang, F.: Applications of molecular dynamics simulation in structure prediction of peptides and proteins. *Computational and structural biotechnology journal* **17**, 1162–1170 (2019)

[22] Germaschewski, K., Fox, W., Abbott, S., Ahmadi, N., Maynard, K., Wang, L., Ruhl, H., Bhattacharjee, A.: The plasma simulation code: A modern particle-in-cell code with patch-based load-balancing. *Journal of Computational Physics* **318**, 305–326 (2016)

[23] Goodfellow, I., Pouget-Abadie, J., Mirza, M., Xu, B., Warde-Farley, D., Ozair, S., Courville, A., Bengio, Y.: Generative adversarial nets. In: *NeurIPS* (2014)

[24] Ho, J., Jain, A., Abbeel, P.: Denoising diffusion probabilistic models. In: *NeurIPS* (2020)

[25] Ho, J., Saharia, C., Chan, W., Fleet, D.J., Norouzi, M., Salimans, T.: Cascaded diffusion models for high fidelity image generation. *Journal of Machine Learning Research* **23**(47), 1–33 (2022)

[26] Imani, Z., Aeron, S., Wongjirad, T.: Score-based diffusion models for generating liquid argon time projection chamber images (2024)

[27] Jiang, C., Schroeder, C., Selle, A., Teran, J., Stomakhin, A.: The affine particle-in-cell method. *ACM Transactions on Graphics (TOG)* **34**(4), 1–10 (2015)

[28] Keefe, D.: Inertial confinement fusion. *Annual Review of Nuclear and Particle Science* **32**(1), 391–441 (1982)

[29] Kemp, A.J., Pfund, R.E., Meyer-ter Vehn, J.: Modeling ultrafast laser-driven ionization dynamics with monte carlo collisional particle-in-cell simulations. *Physics of Plasmas* **11**(12), 5648–5657 (2004)

[30] Kingma, D.P., Ba, J.: Adam: A method for stochastic optimization. In: *ICLR* (2015)

- [31] Kingma, D.P., Welling, M.: Auto-encoding variational bayes. arXiv preprint arXiv:1312.6114 (2013)
- [32] Klimo, O., Weber, S., Tikhonchuk, V., Limpouch, J.: Particle-in-cell simulations of laser–plasma interaction for the shock ignition scenario. *Plasma Physics and Controlled Fusion* **52**(5), 055013 (2010)
- [33] Kong, X., Huang, M.C., Ren, C., Decyk, V.K.: Particle-in-cell simulations with charge-conserving current deposition on graphic processing units. *Journal of Computational Physics* **230**(4), 1676–1685 (2011)
- [34] Kube, R., Churchill, R., Sturdevant, B.: Machine learning accelerated particle-in-cell plasma simulations. arXiv preprint arXiv:2110.12444 (2021)
- [35] Langdon, A.B.: Evolution of particle-in-cell plasma simulation. *IEEE Transactions on Plasma Science* **42**(5), 1317–1320 (2014)
- [36] Lange, R.: Adpic—a three-dimensional particle-in-cell model for the dispersal of atmospheric pollutants and its comparison to regional tracer studies. *Journal of Applied Meteorology and Climatology* **17**(3), 320–329 (1978)
- [37] Lewis, H.R., Sykes, A., Wesson, J.: A comparison of some particle-in-cell plasma simulation methods. *Journal of Computational Physics* **10**(1), 85–106 (1972)
- [38] Li, L., Carver, R., Lopez-Gomez, I., Sha, F., Anderson, J.: Generative emulation of weather forecast ensembles with diffusion models. *Science Advances* **10**(13), eadk4489 (2024)
- [39] Liewer, P.C., Decyk, V.K.: A general concurrent algorithm for plasma particle-in-cell simulation codes. *Journal of Computational Physics* **85**(2), 302–322 (1989)
- [40] Liu, X., Gong, C., Liu, Q.: Flow straight and fast: Learning to generate and transfer data with rectified flow (2022)
- [41] Liu, X., Zhang, X., Ma, J., Peng, J., Liu, Q.: Instaflow: One step is enough for high-quality diffusion-based text-to-image generation (2024)
- [42] Markwick, P.R., McCammon, J.A.: Studying functional dynamics in bio-molecules using accelerated molecular dynamics. *Physical Chemistry Chemical Physics* **13**(45), 20053–20065 (2011)
- [43] Nichol, A., Dhariwal, P., Ramesh, A., Shyam, P., Mishkin, P., McGrew, B., Sutskever, I., Chen, M.: Glide: Towards photorealistic image generation and editing with text-guided diffusion models. In: NeurIPS (2021)
- [44] Oyama, N., Ishizaki, N.N., Koide, S., Yoshida, H.: Deep generative model super-resolves spatially correlated multiregional climate data. *Scientific Reports* **13**(1), 5992 (2023)
- [45] Paszke, A., Gross, S., Massa, F., Lerer, A., Bradbury, J., Chanan, G., Killeen, T., Lin, Z., Gimelshein, N., Antiga, L., et al.: Pytorch: An imperative style, high-performance deep learning library. In: NeurIPS (2019)
- [46] Petersen, M., Roig, G., Covino, R.: Dynamicsdiffusion: Generating and rare event sampling of molecular dynamic trajectories using diffusion models. In: NeurIPS 2023 AI for Science Workshop (2023)
- [47] Pritchett, P.L.: Particle-in-cell simulation of plasmas—a tutorial. *Space Plasma Simulation* pp. 1–24 (2003)
- [48] Pukhov, A., Meyer-ter Vehn, J.: Relativistic laser-plasma interaction by multi-dimensional particle-in-cell simulations. *Physics of Plasmas* **5**(5), 1880–1886 (1998)
- [49] Ramesh, A., Dhariwal, P., Nichol, A., Chu, C., Chen, M.: Hierarchical text-conditional image generation with clip latents. arXiv preprint arXiv:2204.06125 **1**(2), 3 (2022)

[50] Rombach, R., Blattmann, A., Lorenz, D., Esser, P., Ommer, B.: High-resolution image synthesis with latent diffusion models. In: CVPR (2022)

[51] Ronneberger, O., Fischer, P., Brox, T.: U-net: Convolutional networks for biomedical image segmentation. In: MICCAI (2015)

[52] Saharia, C., Chan, W., Saxena, S., Li, L., Whang, J., Denton, E.L., Ghasemipour, K., Gontijo Lopes, R., Karagol Ayan, B., Salimans, T., et al.: Photorealistic text-to-image diffusion models with deep language understanding. In: NeurIPS (2022)

[53] Sentoku, Y., Mima, K., Kojima, S.i., Ruhl, H.: Magnetic instability by the relativistic laser pulses in overdense plasmas. *Physics of Plasmas* **7**(2), 689–695 (2000)

[54] Shah, H., Kamaria, S., Markandeya, R., Shah, M., Chaudhury, B.: A novel implementation of 2d3v particle-in-cell (pic) algorithm for kepler gpu architecture. In: 2017 IEEE 24th International Conference on High Performance Computing (HiPC). pp. 378–387. IEEE (2017)

[55] Smith, M.J., Geach, J.E., Jackson, R.A., Arora, N., Stone, C., Courteau, S.: Realistic galaxy image simulation via score-based generative models. *Monthly Notices of the Royal Astronomical Society* **511**(2), 1808–1818 (Jan 2022)

[56] Sohl-Dickstein, J., Weiss, E., Maheswaranathan, N., Ganguli, S.: Deep unsupervised learning using nonequilibrium thermodynamics. In: ICML (2015)

[57] Song, J., Meng, C., Ermon, S.: Denoising diffusion implicit models. ICLR (2021)

[58] Song, Y., Dhariwal, P., Chen, M., Sutskever, I.: Consistency models. In: ICML (2023)

[59] Song, Y., Ermon, S.: Generative modeling by estimating gradients of the data distribution. In: NeurIPS (2019)

[60] Strozzi, D., Tabak, M., Larson, D., Divol, L., Kemp, A., Bellei, C., Marinak, M., Key, M.: Fast-ignition transport studies: Realistic electron source, integrated particle-in-cell and hydrodynamic modeling, imposed magnetic fields. *Physics of Plasmas* **19**(7) (2012)

[61] Sulsky, D., Zhou, S.J., Schreyer, H.L.: Application of a particle-in-cell method to solid mechanics. *Computer physics communications* **87**(1-2), 236–252 (1995)

[62] Suzuki, J., Shimazu, H., Fukazawa, K., Den, M.: Acceleration of pic simulation with gpu. *Plasma and Fusion Research* **6**, 2401075–2401075 (2011)

[63] Taccogna, F., Minelli, P.: Pic modeling of negative ion sources for fusion. *New Journal of Physics* **19**(1), 015012 (2017)

[64] Tskhakaya, D., Matyash, K., Schneider, R., Taccogna, F.: The particle-in-cell method. *Contributions to Plasma Physics* **47**(8-9), 563–594 (2007)

[65] Vaswani, A., Shazeer, N., Parmar, N., Uszkoreit, J., Jones, L., Gomez, A.N., Kaiser, Ł., Polosukhin, I.: Attention is all you need. In: NeurIPS (2017)

[66] Verboncoeur, J.P.: Particle simulation of plasmas: review and advances. *Plasma Physics and Controlled Fusion* **47**(5A), A231 (2005)

[67] Wang, P., Zhu, X.: Hybrid cpu-and gpu-based implementation for particle-in-cell simulation on multicore and multi-gpu systems. In: 2021 Photonics & Electromagnetics Research Symposium (PIERS). pp. 155–161. IEEE (2021)

[68] Wilks, S.: Simulations of ultraintense laser–plasma interactions. *Physics of Fluids B: Plasma Physics* **5**(7), 2603–2608 (1993)

[69] Wu, F., Li, S.Z.: Diffmd: a geometric diffusion model for molecular dynamics simulations. In: AAAI (2023)

[70] Xu, M., Chen, F., Liu, X., Ge, W., Li, J.: Discrete particle simulation of gas–solid two-phase flows with multi-scale cpu–gpu hybrid computation. *Chemical engineering journal* **207**, 746–757 (2012)

SUMMARY OF THE APPENDIX

This supplementary contains additional experimental results and discussions of our NeurIPS 2024 submission: DIFF-PIC: *Revolutionizing Particle-In-Cell Simulation for Advancing Nuclear Fusion with Diffusion Models*, organized as follows:

- §S1 reports the **Implementation Details** of our experiments.
- §S2 presents an **Ablation Study** over our proposed modules (§3.2 and §3.3).
- §S3 discusses the **Social Impact and Limitation** of our research.
- §S4 elaborates the **Ethical Safeguard** of our dataset.
- §S5 affirms the **Reproducibility** of our approach.
- §S6 provides the **Data License** pertaining to the methods employed for comparative analysis.

S1 Implementation Details

Experimental Configurations. The comprehensive schematic of DIFF-PIC is depicted in Fig.2. The architectural foundation of our model is predicated on the U-Net framework [51], incorporating a series of three down-sampling blocks followed by three up-sampling blocks. The training regimen of our model encompasses an extensive 600 epochs, employing a batch size of 64, a configuration empirically validated to secure model convergence. Furthermore, the training protocol adheres to a fixed learning rate of 0.0005, optimized via the Adam optimizer[30]. The optimization objective is formulated as delineated in Eq. 7.

Physically-Informed Condition Encoder. We employ a quartet of distinct condition encoders, each tailored to a specific type of condition. Apart from the encoder addressing the designated snapshot t_{as} , the remaining three encoders share an identical architectural framework, albeit undergoing separate training processes. Specifically, the positional encoding mechanism yields a 16-dimensional embedding from a single input. The polynomial encoder operates with a maximum polynomial degree of 4. Subsequently, a single-layer MLP module processes the concatenation of outputs from both the positional and polynomial encoders to further refine the learned embedding, preserving its dimensionality. Notably, the architecture for the snapshot encoder mirrors this design, excluding the polynomial encoder component.

Rectified Flow-based Acceleration. We adhere to the theoretical framework proposed in [40] to refine the denoising trajectory (see Eq. 7) of DIFF-PIC. Additionally, we further streamline the learned trajectories by applying the reflow technique, thereby transforming our model into a one-step conditional diffusion model.

S2 Ablation Study

This section provides an in-depth analysis of the systemic design of DIFF-PIC through an ablation study. By systematically removing or altering components of the model, we aim to isolate and understand the contributions of each part to the overall performance.

Table S1: A set of **ablation studies** regarding interpolation evaluation over Testing Set for E1.

Encoder	FID \downarrow	SWD \downarrow	MMD \downarrow	Acceleration	FID \downarrow	SWD \downarrow	MMD \downarrow	# of Samples	FID \downarrow	SWD \downarrow	MMD \downarrow
B-1	1.87 \pm 0.12	46.8 \pm 2.7	7.21e-4	B-2	1.54 \pm 0.03	44.3 \pm 1.4	5.11e-4	200	2.85 \pm 0.36	67.4 \pm 5.8	9.46e-4
Conv layer	1.92 \pm 0.08	45.5 \pm 2.5	7.48e-4	DDIM	3.79 \pm 0.24	76.5 \pm 6.1	2.14e-3	500	2.18 \pm 0.17	55.3 \pm 2.9	8.17e-4
W/O	1.96 \pm 0.09	47.4 \pm 1.8	7.59e-4	ODE only	1.60 \pm 0.07	41.3 \pm 1.5	5.33e-4	700	1.62 \pm 0.05	40.4 \pm 1.1	5.35e-4
Ours	1.62 \pm 0.05	40.4 \pm 1.1	5.35e-4	Ours	1.62 \pm 0.05	40.4 \pm 1.1	5.35e-4	1000	1.63 \pm 0.04	40.2 \pm 1.3	5.32e-4

(a) PICE in §3.2

(b) RFA in §3.3

(c) Sparse sampling

Physically-Informed Condition Encoder. This study provides a comprehensive evaluation of the efficacy of our Physically-Informed Condition Encoder by juxtaposing it with a baseline model. The baseline model employs a straightforward encoder consisting of a naive MLP layer, augmented by Rectified Flow-based Acceleration. The performance metrics for this baseline model are presented in Table S1a, showcasing FID, SWD, and MMD scores of 1.87, 46.8, and 7.21e-4, respectively. To examine the impact of the encoder architecture on model performance, we first replaced the naive

MLP layer with convolutional layers. This modification resulted in the model achieving FID, SWD, and MMD scores of 1.92, 45.5, and 7.48e-4, respectively. Furthermore, we try to just concatenate the embeddings from positional encoding and polynomial encoding without further refinement (denoted as W/O). This change yielded FID, SWD, and MMD scores of 1.96, 47.4, and 7.59e-4, respectively. The most significant performance gains were observed when we integrated our Physically-Informed Condition Encoder into the model. This advanced encoder leverages polynomial basis functions to incorporate physical insights into the encoding process. The inclusion of these physically-informed features enabled the model to achieve superior performance with FID, SWD, and MMD scores of **1.62, 40.4, and 5.35e-4**, respectively.

These results highlight several critical observations. Firstly, utilizing learnable polynomial architectures, specifically transformation functions constructed as a linear combination of polynomial basis functions, can enhance performance. Secondly, the exceptional performance of the Physically-Informed Condition Encoder underscores the value of integrating domain-specific knowledge into the model architecture. By incorporating physical principles directly into the encoding process, the encoder provides more informative and relevant features, significantly enhancing the model’s ability to generate high-quality outputs. These findings clearly indicate that the Physically-Informed Condition Encoder plays a pivotal role in our approach. Its ability to incorporate physical insights directly into the model not only improves individual performance metrics but also profoundly impacts the overall efficacy of the model. This underscores the potential for further exploration and application of physically-informed methods in various modeling and prediction tasks.

Rectified Flow-based Acceleration. We next study the influence of the RFA module in Table S1b. The baseline for our analysis is B-2 (see §4.1), which is a version of DIFF-PIC that uses 1000 denoising steps through the DDPM noise scheduler [24]. Under this configuration, the baseline model achieves an FID score of 1.54, an SWD score of 44.3, and an MMD score of 5.11e-4. When the noise scheduler is substituted with DDIM [57], the performance exhibits 3.79 for FID, 76.5 for SWD, and 2.14e-3 for MMD. In an alternative scenario where only the Ordinary Differential Equation (ODE) method is employed (without reflow procedure), the results show 1.60 for FID, 41.3 for SWD, and 5.33e-4 for MMD. Implementing our proposed RFA approach yields a performance of **1.62** for FID, **40.4** for SWD, and **5.35e-4** for MMD. It is noteworthy that while the baseline model B-2 demonstrates superior performance in terms of FID and MMD, our RFA approach significantly outperforms it in terms of runtime efficiency, achieving a speedup factor of 10^4 (refer to Table 4 for detailed runtime comparisons).

Sparse Sampling. Lastly, we extend our investigative efforts to scrutinize the influence of varying the number of samples on sparse sampling efficacy. As delineated in Table S1c, our methodology exhibits commendable performance across multiple evaluative metrics, including FID, SWD, and MMD. The performance metrics span from 1.62 to 2.85 for FID, 40.4 to 67.4 for SWD, and 5.32e-4 to 9.46e-4 for MMD, respectively. These results were obtained by incrementally adjusting the sample size from 200 to 1000. A salient observation from our experiments is the model’s performance convergence at 700 samples. This convergence suggests that using 700 samples strikes an optimal balance between computational efficiency and effectiveness. The diminishing returns observed beyond this point indicate that further increases in sample size do not yield proportionate improvements in performance metrics. Consequently, we adopt 700 samples as the default configuration for our approach.

S3 Social Impacts & Limitation

The advent of DIFF-PIC heralds a substantial breakthrough in the synthesis of PIC simulations with diffusion model paradigms, significantly augmenting predictive capabilities in the realm of ICF. This pioneering approach has demonstrated commendable performance metrics. From a societal vantage point, the ramifications of DIFF-PIC are profoundly advantageous, as our approach furnishes a pivotal instrument for advancing our comprehension and proficiency in exploiting fusion energy — an endeavor that holds promise as a cornerstone for long-term sustainable energy solutions.

Nonetheless, it is crucial to recognize and meticulously evaluate the potential negative impact and limitations inherent in this technology. Analogous to other generative models, DIFF-PIC encounters challenges when addressing corner cases, which may not be adequately represented in the training data. This limitation accentuates the necessity for continuous research and refinement, particularly in its application to real-world ICF scenarios where unforeseen behaviors may manifest. Therefore, despite

the model’s promising applications, its implementation in practical contexts must be approached with prudence, ensuring ongoing assessment and adaptation to uphold reliability and safety in its generative outputs.

S4 Ethical Safeguards

In our study, which introduces a novel dataset, we will implement comprehensive ethical safeguards to mitigate potential misuse and ensure responsible utilization, as detailed in the protocols included in the final release of models and datasets. These protocols encompass strict usage guidelines, access restrictions, the incorporation of safety filters, and monitoring mechanisms. We perform thorough risk assessments to identify potential misuse scenarios and develop tailored mitigation strategies, such as robust data governance frameworks. While not all research may necessitate stringent safeguards, we adhere to best practices, promoting ethical awareness and encouraging researchers to consider the broader impacts of their work. Additionally, we maintain detailed documentation for transparency and accountability for the data we release. These efforts underscore our commitment to upholding the highest standards of conduct in scientific inquiry, aiming to protect the interests of involved parties.

S5 Reproducibility

DIFF-PIC is implemented using PyTorch [45]. PIC simulations are executed on the Perlmutter supercomputer, located at the National Energy Research Scientific Computing (NERSC) facility, utilizing AMD EPYC 7763 CPUs. The experimental procedures for **DIFF-PIC** are conducted on an Nvidia RTX 4090 GPU in conjunction with an Intel 13th Gen i9-13900KF CPU. To ensure reproducibility, the complete implementation will be made publicly available upon acceptance.

S6 Licenses for existing assets

Most of the methods utilized for comparison in our study are reproduced by ourselves. The PIC Simulation is implemented based on the publicly available version at **OSIRIS**, and is distributed under the AGPL-3.0 license.